DEVELOPMENTAL DYNAMICS 240:384–393, 2011

RESEARCH ARTICLE

The Chemokine Receptor CXCR7 Functions to Regulate Cardiac Valve Remodeling

Sangho Yu,[1,2,3†] Dianna Crawford,[4†,‡] Takatoshi Tsuchihashi,[1,2,3§] Timothy W. Behrens,[4#] and Deepak Srivastava[1,2,3]*

CXCR7 (RDC1), a G-protein-coupled receptor with conserved motifs characteristic of chemokine receptors, is enriched in endocardial and cushion mesenchymal cells in developing hearts, but its function is unclear. *Cxcr7* germline deletion resulted in perinatal lethality with complete penetrance. Mutant embryos exhibited aortic and pulmonary valve stenosis due to semilunar valve thickening, with occasional ventricular septal defects. Semilunar valve mesenchymal cell proliferation increased in mutants from embryonic day 14 onward, but the cell death rate remained unchanged. *Cxcr7* mutant valves had increased levels of phosphorylated Smad1/5/8, indicating increased BMP signaling, which may partly explain the thickened valve leaflets. The hyperproliferative phenotype appeared to involve *Cxcr7* function in endocardial cells and their mesenchymal derivatives, as *Tie2-Cre Cxcr7*$^{flox/-}$ mice had semilunar valve stenosis. Thus, CXCR7 is involved in semilunar valve development, possibly by regulating BMP signaling, and may contribute to aortic and pulmonary valve stenosis. *Developmental Dynamics 240:384–393, 2011*.

Key words: CXCR7; G-protein coupled receptor; chemokine receptor; endocardial cells; cardiac valve remodeling; semilunar valve development; BMP signaling

Accepted 17 December 2010

INTRODUCTION

CXCR7 (RDC1) is an evolutionarily conserved, seven-transmembrane G-protein-coupled receptor (GPCR) with motifs characteristic of chemokine receptors, such as the DRY motif. It is expressed in brain, heart, kidney, spleen, thymus, and various tumors and associated vascular endothelial cells (Heesen et al., 1998; Madden et al., 2004; Burns et al., 2006; Miao et al., 2007). CXCR7 binds to CXCL12 (SDF-1) with high affinity (Balabanian et al., 2005; Burns et al., 2006), challenging the notion that CXCL12 has a monogamous relationship with CXCR4, as suggested by the nearly identical phenotypes of CXCL12 and CXCR4 knockout mice (Nagasawa et al., 1996; Ma et al., 1998; Tachibana et al., 1998; Zou et al., 1998). CXCR7 also binds to another chemokine, CXCL11 (I-TAC) (Burns et al., 2006). However, the significance of ligand binding to CXCR7 is unclear, since CXCR7 does not appear to transduce any intracellular signaling, such as Ca^{2+} mobilization or mitogen-activated protein kinase (MAPK) signaling, which are the hallmarks of chemokine receptor activation (Burns et al., 2006; Proost et al., 2007; Boldajipour et al., 2008; Hartmann et al., 2008).

Despite the lack of ligand-mediated signaling, expression of and ligand binding to CXCR7 has significant cellular and physiological consequences. During CXCR4-mediated migration of primordial germ cells (Boldajipour et al., 2008) and lateral line

[1]Gladstone Institute of Cardiovascular Disease, San Francisco, California
[2]Department of Biochemistry & Biophysics, University of California, San Francisco, California
[3]Department of Pediatrics, University of California, San Francisco, California
[4]Center for Immunology, Department of Medicine, University of Minnesota Medical School, University of Minnesota, Minneapolis, Minnesota
[†]Sangho Yu and Dianna Crawford contributed equally to this work.
[‡]D. Crawford's present address is Amgen Inc., One Amgen Center Drive, Thousand Oaks, CA 91320.
[§]T. Tsuchihashi's present address is Division of Cardiology, Department of Pediatrics, School of Medicine, Keio University, 35 Shinanomachi Shinjuku-ku, Tokyo, Japan 160-8582.
[#]T.W. Behrens's present address is Genentech Inc., 1 DNA Way, South San Francisco, CA 94080.
***Correspondence to: Deepak Srivastava, Gladstone Institute of Cardiovascular Disease, 1650 Owens Street, San Francisco, CA 94158. E-mail: dsrivastava@gladstone.ucsf.edu**

DOI 10.1002/dvdy.22549
Published online 19 January 2011 in Wiley Online Library (wileyonlinelibrary.com).

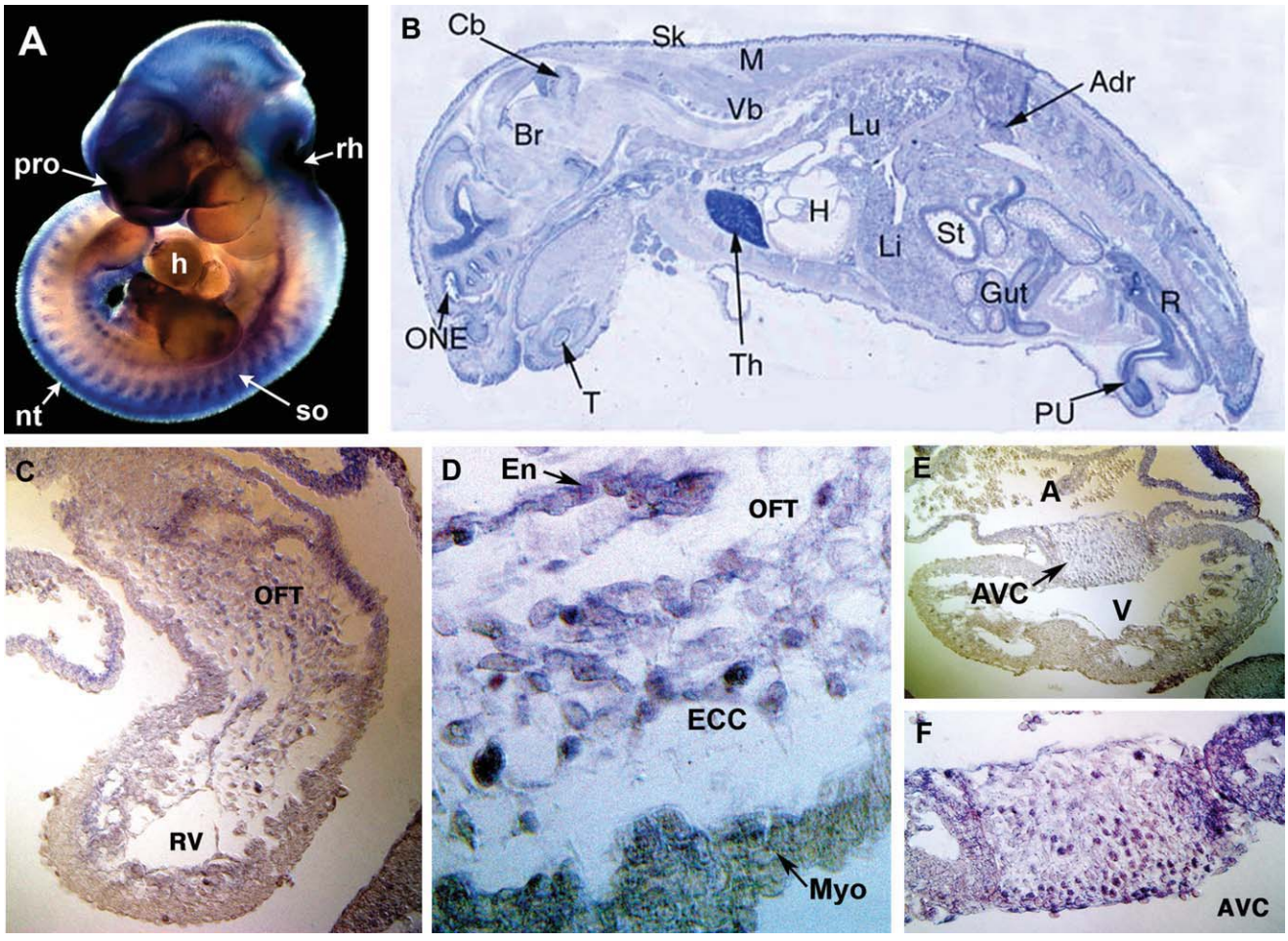

Fig. 1. Expression pattern of *Cxcr7* mRNA in developing mouse heart. **A:** Whole-mount in situ hybridization was carried out with digoxigenin (DIG)-labeled *Cxcr7* riboprobe at E10.5. *Cxcr7* mRNA is expressed in the prosencephalon, rhombencephalon, somites, neural tube, and heart. h, heart; nt, neural tube; pro, prosencephalon; rh, rhomboencephalon; so, somite. **B:** Section in situ hybridization image of sagittally sectioned P1 mouse. *Cxcr7* is expressed in various tissues, including brain, thymus, heart, stomach, and liver. Adr, adrenal gland; Br, brain; Cb, cerebellum; H, heart; Li, liver; Lu, lung; M, muscle; ONE, optic nerve ending; PU, penile urethra; R, rectum; Sk, skin; St, stomach; T, tooth; Th, thymus; Vb, vertebrae. **C–F:** Transverse sections made after whole-mount in situ hybridization. *Cxcr7* is expressed in endocardial cells and endocardial cushion mesenchymal cells in both outflow tract (OFT) and atrioventricular canal (AVC) regions. Its expression in myocardial cells is much weaker than that of endocardial cells. D and F are high-magnification images of OFT and AVC endocardial cushion regions, respectively. En, endocardium; ECC, endocardial cushion; Myo, myocardium; A, atrium; V, ventricle; RV, right ventricle.

primordium (Dambly-Chaudiere et al., 2007; Valentin et al., 2007) in zebrafish, CXCR7 creates an essential CXCL12 gradient by sequestering and internalizing CXCL12. CXCR7 forms a heterodimer with CXCR4 and modulates certain aspects of its function (Sierro et al., 2007; Hartmann et al., 2008; Kalatskaya et al., 2009; Levoye et al., 2009). CXCR7 is also important in CXCR4-mediated transendothelial migration of tumor cells, but not in intra-tissue chemotaxis (Zabel et al., 2009). Overall, CXCR7 is an atypical chemokine receptor that does not directly activate downstream pathways, but rather modifies or fine-tunes the activation of CXCR4 in response to CXCL12. In certain environments, CXCR7 may also have CXCR4-independent functions, as it promotes cell survival and adhesion even without ligand binding; the mechanism is unknown (Raggo et al., 2005; Burns et al., 2006; Miao et al., 2007).

Cardiac valve morphogenesis is a complicated and delicate process involving myriad signaling events (Armstrong and Bischoff, 2004). We found that CXCR7 is expressed in developing and adult heart, especially in endocardial cells and their mesenchymal derivatives. Given the complementary expression pattern of CXCR4 and CXCL12 in the heart and their identical loss-of-function cardiac phenotypes in mice, we speculated that CXCR7 is important for cardiac development. The consequences of CXCR7 deletion have been reported by two groups, but the phenotypes have been divergent, leaving its function in vivo unclear, particularly regarding CXCR7's effects on cardiac development.

In this study, we generated *Cxcr7* floxed mice and characterized the global and cell-specific consequences of complete loss of *Cxcr7* function. Complete deletion of *Cxcr7* produced perinatal lethality due to enlarged semilunar (aortic and pulmonary) valves and occasional ventricular septal defects

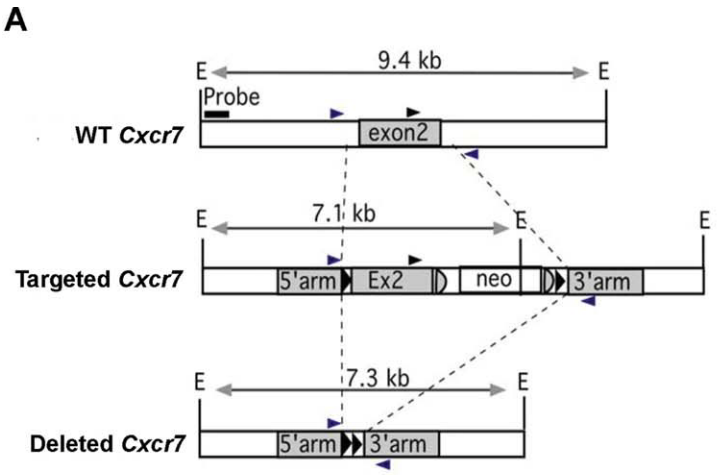

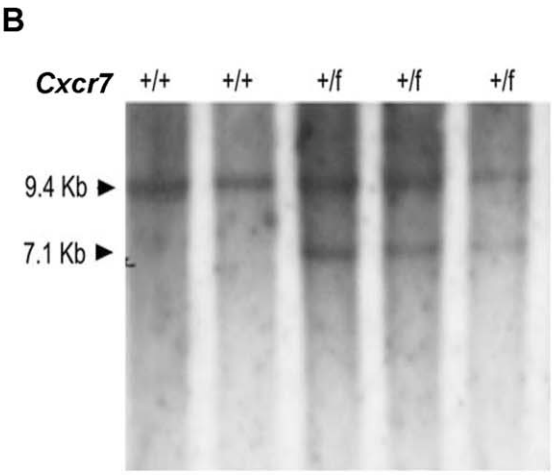

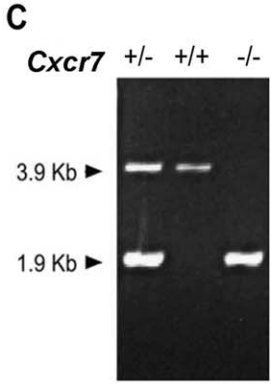

D

3 wks	+/+	+/-	-/-
number	25	44	0
%	36%	64%	0%

E16.5	+/+	+/-	-/-
number	12	21	10
%	28%	49%	23%

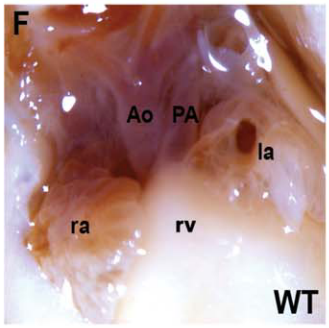

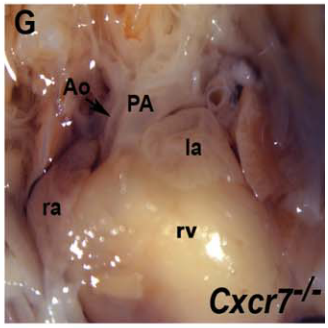

Fig. 2. Generation of targeted *Cxcr7*-null mice. **A:** Schematic representation of the wild-type *Cxcr7* locus, the targeted allele, and the deleted locus. Shaded regions represent exon 2 (exon 2, top); the cloning fragment that includes exon 2 and about 100 bp up- and downstream of exon 2 (Ex2, middle); the 5′ homologous arm, which was cloned from DNA immediately upstream of Ex2 (5′ arm, middle and lower); and the 3′ homologous arm, which was cloned from DNA immediately downstream of Ex2 (3′ arm, middle and lower). Black triangles indicate *LoxP* sites; arrowhead indicates primer sites used for genotyping. E, EcoRV; neo, neomycin-resistance gene cassette. **B:** Southern blot analysis of ES cell clones showing non-targeted (+/+) and targeted (+/*flox*) clones. The 9.4-kb wild-type and 7.1-kb targeted allele fragments digested with EcoRV (E) were identified with an upstream probe, as shown in A. **C:** PCR analysis of genomic DNA from E16.5 wild-type (+/+) embryos or embryos heterozygous (+/−) or homozygous (−/−) for Cre-mediated deletion of the targeted locus. The 3.9-kb wild-type and 1.9-kb deleted products were from a single set of primers outside of exon 2, as shown in A. **D:** Genotypes of offspring from $Cxcr7^{+/-} \times Cxcr7^{+/-}$ crosses at weaning and at E16.5. **E:** Six of eight E18.5 mice from a single ($Cxcr7^{+/-} \times Cxcr7^{+/-}$) litter, photographed less than 1 hr after cesarean birth. Identifier and genotypes are shown for each mouse. **F,G:** Frontal views of E18.5 wild-type and $Cxcr7^{-/-}$ hearts. In some $Cxcr7^{-/-}$ hearts (22%), the aorta was misaligned and displaced to the right side (arrow). Ao, aorta; PA, pulmonary artery; ra, right atrium; la, left atrium; rv, right ventricle.

(VSDs). Endothelial-specific deletion of *Cxcr7* mediated by *Tie2-Cre* caused a similar, but less severe, cardiac phenotype. The valve defects were due to increased proliferation of valve mesenchymal cells associated with increased bone morphogenetic protein (BMP) signaling. Our results suggest that CXCR7 is required for proper cardiac semilunar valve morphogenesis and normal BMP signaling.

RESULTS

Expression Pattern of CXCR7 in Mice

To examine the expression pattern of CXCR7 in the embryonic heart, we performed whole-mount in situ hybridization. In E10.5 mouse embryos, *Cxcr7* was expressed at high levels in the prosencephalon, especially in the nasal process, and in a part of the rhomboencephalon and at lower levels in the neural tube, somites, and heart (Fig. 1A). A similar pattern was observed in postnatal day 1 (P1) mice (Fig. 1B). In E10.5 heart, *Cxcr7* was mainly expressed in endocardial cells and their endocardial cushion mesenchymal cell derivatives, in both the outflow tract (OFT) and atrioventricular canal (AVC) regions (Fig. 1C–F) and to a lesser degree in myocardial cells (Fig. 1C,E). A portion of OFT cushion mesenchymal cells are also derived from cardiac neural crest cells and they also seemed to express *Cxcr7* since all OFT cushion cells were $Cxcr7^{+}$, even though neural crest cells did not express *Cxcr7*.

Perinatal Lethality of *Cxcr7*-Deficient Mice

To test the function of CXCR7 in mice, we generated mice with *loxP* sites flanking the *Cxcr7* gene ($Cxcr7^{flox/flox}$) and used them to create ubiquitous or endothelial cell-specific *Cxcr7* knockout mice. A targeting vector was generated to insert *loxP* sequences immediately upstream and downstream of *Cxcr7* exon 2 by homologous recombination with the *Cxcr7* locus (Fig. 2A). Removal of exon 2, which contains the entire coding region of *Cxcr7*, by Cre-mediated recombination would result in the complete loss of CXCR7 function. After confirmation by Southern blot, correctly targeted embryonic stem cell clones (Fig. 2B) were injected into blastocysts. Chimeric offspring were crossed with wild-type C57BL/6 mice to generate $Cxcr7^{flox}$ mice, which were bred with *deleter* transgenic mice (Schwenk et al., 1995) to allow Cre-mediated recombination in all cells. F1 mice were out-crossed with wild-type C57BL/6 mice to establish a stably transmitting mouse line with heterozygous deletion of *Cxcr7* exon 2 ($Cxcr7^{+/-}$) (Fig. 2C).

When $Cxcr7^{+/-}$ mice were intercrossed, no $Cxcr7^{-/-}$ mice were found at weaning (Fig. 2D). A normal Mendelian ratio was observed at E16.5 (Fig. 2D) without abnormalities in size, color, or gross anatomy. About a third of E18.5 $Cxcr7^{-/-}$ mice delivered by cesarean birth at E18 were dead. The remaining mice died shortly after birth; most were cyanotic and gasped for breath, but the phenotype was variable. For example, in a litter of eight mice, one of three $Cxcr7^{-/-}$ mice died at or just before birth and appeared to have a catastrophic circulatory failure in late development, as it was completely white within a blood-filled embryonic sac (mouse 18-12, Fig. 2E). The second appeared anatomically normal but never breathed (mouse 18-10, Fig. 2E). And the third gasped and remained cyanotic before dying within 1 hr after birth (mouse 18-6, Fig. 2E). Some $Cxcr7^{-/-}$ mice appeared normal and robust at birth but then showed signs of stress, such as gasping for breath, and died suddenly.

CXCR7 Deficiency Causes Thickening of Semilunar Valves and Ventricular Septal Defect

To analyze the phenotypes of $Cxcr7^{-/-}$ mice in detail, we harvested E18.5 embryos from intercrosses of $Cxcr7^{+/-}$ mice, and examined the internal organs. In $Cxcr7^{-/-}$ embryos, the lungs appeared normal and were able to inflate. All other internal organs looked grossly normal except the hearts, which were slightly larger than age-matched wild-type hearts and occasionally had dilated atria or malalignment of the aorta (Fig. 2F,G).

Transverse and coronal sections of E18.5 $Cxcr7^{-/-}$ hearts revealed thickened semilunar valves (pulmonary and aortic valves) in all embryos; atrioventricular (tricuspid and mitral) valves were normal (Fig. 3A–J). One third of the embryos (n=9) had VSDs in the membranous portion of the septum, and 22% had overriding aortas (Fig. 3I). In contrast to a previous report (Sierro et al., 2007), we did not observe atrial septal defects or bicuspid semilunar valves. The perinatal lethality most likely resulted from insufficient blood flow to the body caused by semilunar valve stenosis, a condition that can cause severe cardiac dysfunction in human newborns as well.

To determine when the semilunar valve thickening occurred during development, heart sections were made at progressive mouse embryonic stages. Until around E14.0, there was no apparent difference in the size of the OFT endocardial cushions (Fig. 3K–M and O–Q). However, at E15.5, when wild-type valve thinning into leaflets had already begun, $Cxcr7^{-/-}$ pulmonary and aortic valves were still thick, indicating defects in semilunar valve remodeling (Fig. 3N,R). Mitral and tricuspid valves were normal in mutants. Since OFT endocardial cushion is composed of both endocardial- and neural crest–derived cells, while AVC endocardial cushion is almost exclusively derived from endocardial cells (Hutson and Kirby, 2007; Snarr et al., 2008), this result may reflect function of *Cxcr7* in both cell types.

Increased Cell Proliferation in Semilunar Valves of $Cxcr7^{-/-}$ Embryos

Some neural crest cells originating at the level of the posterior rhombencephalon migrate to the heart through pharyngeal arches 3, 4, and 6 and contribute to various developmental events, such as outflow septation, great vessel alignment, and remodeling of pharyngeal arch arteries (Hutson and Kirby, 2003; Stoller and Epstein, 2005). Since valve thickening was observed only in OFT valves, and VSD and overriding aorta were present in some cases, we speculated that CXCR7 is involved in the migration of cardiac neural crest cells. However, whole-mount in situ hybridization for *Crabp1* mRNA, a marker of neural crest cells, at E10.5 did not reveal any gross abnormalities between neural crest migration to

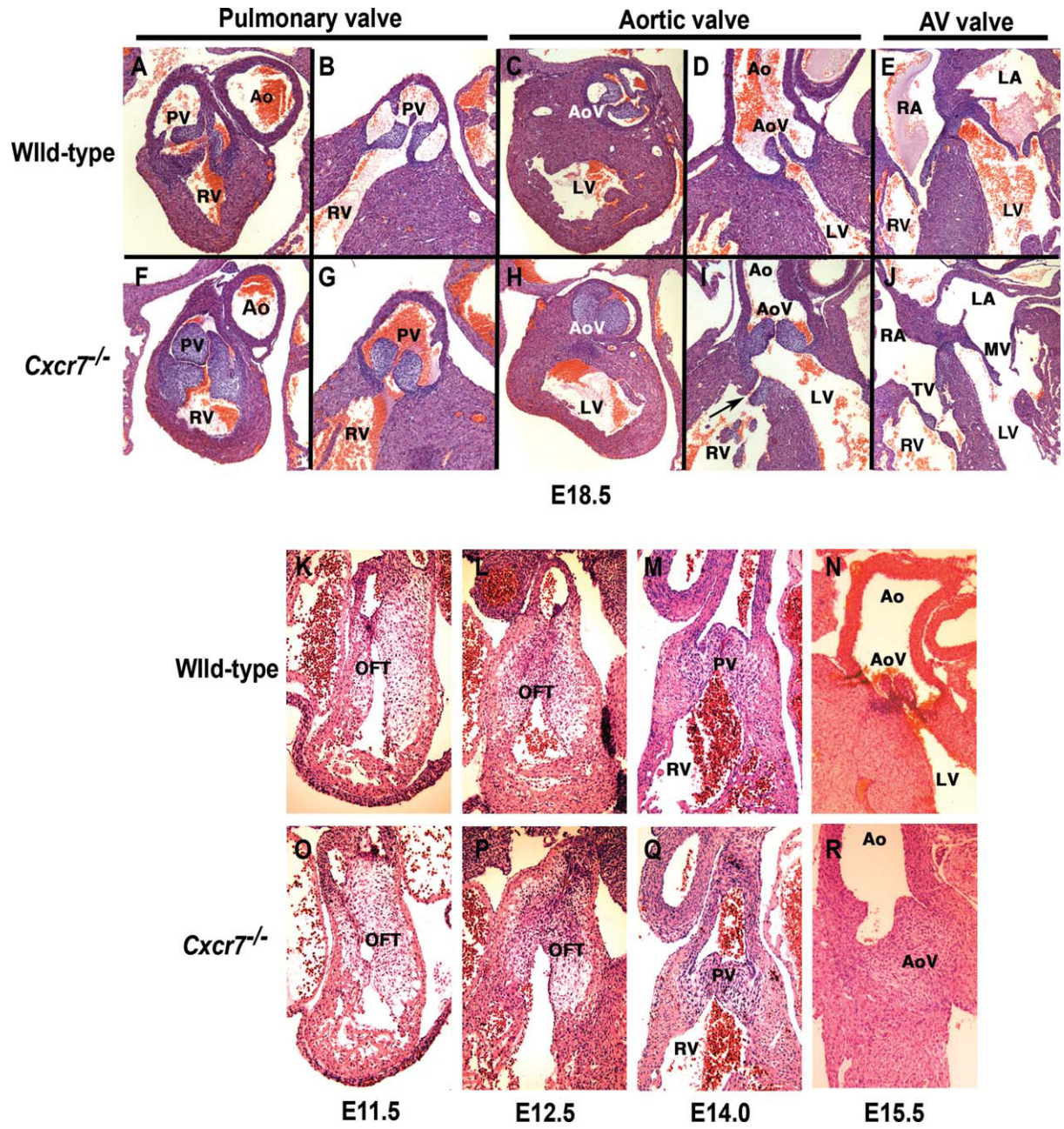

Fig. 3.

pharyngeal arches 3, 4, and 6 in wild-type and *Cxcr7*$^{-/-}$ embryos (data not shown).

To investigate whether the proliferation or apoptosis of semilunar valve mesenchymal cells was affected in *Cxcr7*$^{-/-}$ embryos at various developmental stages, we analyzed cell proliferation by phospho-histone H3 (pH3) immunofluorescence (Fig. 4A,B) and cell death by TUNEL assay. In wild-

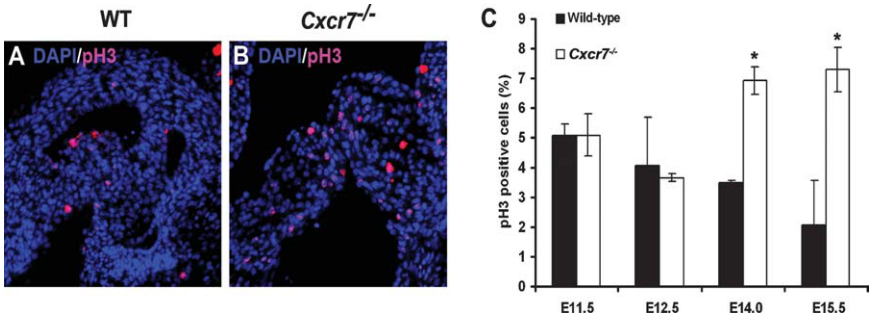

Fig. 4.

type semilunar valves, the percentage of cells undergoing mitosis decreased as embryos grew older. In contrast, *Cxcr7*$^{-/-}$ valves had ~2-fold more pH3-positive semilunar valve cells than wild-type valves at E14.0 and 3.5-fold more at E15.5 (Fig. 4C). No differences were detected in the percentage of pH3-positive cells in pulmonary valves compared to aortic valves. The percentages of cells undergoing apoptosis were almost identical in wild-type and *Cxcr7*$^{-/-}$ valves (data not shown).

CXCR7 in Endocardial Cells Is Important for Semilunar Valve Morphogenesis

To identify the cell type in which CXCR7 functions during valve development and to examine the role of CXCR7 in the adult heart, we deleted *Cxcr7* specifically in endothelial and endocardial cells using the *Tie2-Cre* transgene. *Tie2-CreCxcr7*$^{flox/-}$ mice survived normally after birth and were fertile. However, at 6 months of age, they had marked cardiac hypertrophy (Fig. 5A). Cross-sections of age-matched wild-type and *Tie2-CreCxcr7*$^{flox/-}$ hearts revealed much thicker ventricular walls in mutant hearts, but no difference in the size of the ventricular cavity (Fig. 5B).

Echocardiographic analysis of cardiac function at 6 months of age showed no difference in fractional shortening or ejection fraction between *Tie2-CreCxcr7*$^{flox/-}$ and wild-type mice (data not shown), but the left ventricular posterior wall was about 1.4-fold thicker in *Tie2-CreCxcr7*$^{flox/-}$ mice (Fig. 5C). These features are consistent with concentric hypertrophy caused by pressure overload (Jessup and Brozena, 2003).

To determine whether *Tie2-CreCxcr7*$^{flox/-}$ mice had semilunar valve stenosis, we examined histological sections at the level of the semilunar valves. Indeed, the semilunar valves of *Tie2-CreCxcr7*$^{flox/-}$ mice were thicker than those of wild-type control mice, and the difference was more dramatic in the aortic valves compared to the pulmonary valves (Fig. 5D–G). This result suggests that *Cxcr7* expression in endocardial cells and their valve mesenchymal derivatives is necessary to prevent thickening of the semilunar valves.

Examination of the myocardial structure of *Tie2-CreCxcr7*$^{flox/-}$ hearts at high magnification revealed greatly enlarged cardiomyocytes, cellular disarray, and increased intercellular space (Fig. 5H,I). At 6 months of age, the mutant mice had substantial fibrosis, marked by Masson's trichrome staining, present in the myocardium and around microvessels in the heart; little fibrosis was detected in wild-type mice (Fig. 5J,K).

BMP Signaling Is Enhanced in Semilunar Valves of *Cxcr7* Mutants

A hypomorphic allele of epidermal growth factor receptor (EGFR) also results in thickening of semilunar valves (Chen et al., 2000), and mutation of one of its ligands, heparin-binding epidermal growth factor (HB-EGF), led to dysregulation of BMP signaling and similar valve stenosis in mice (Jackson et al., 2003). To determine whether BMP signaling was increased in *Cxcr7*$^{-/-}$ semilunar valves, we performed immunostaining for phospho-Smad1/5/8 (pSmad1/5/8), which transduces BMP signaling. pSmad1/5/8 levels were about 1.5-fold higher in *Cxcr7*$^{-/-}$ semilunar valves than in wild-type valves throughout development (Fig. 6A–E).

DISCUSSION

This study shows that endothelial expression of the chemokine receptor CXCR7 is important in limiting proliferation of cells during cardiac semilunar valve morphogenesis. *Cxcr7* germline deletion in mice caused perinatal lethality, likely because of insufficient blood supply to peripheral tissues as a result of severe aortic and pulmonary valve thickening and stenosis. Loss of CXCR7 also increased BMP signaling in semilunar valves and caused a sustained high proliferative rate of valve mesenchymal cells during the valve remodeling stage. *Tie2-CreCxcr7*$^{flox/-}$ mice with endothelial cell-specific ablation of *Cxcr7* had similarly enlarged semilunar valves later in life and developed massive cardiac hypertrophy presumably due to aortic valve stenosis.

These results are consistent with the first report of a *Cxcr7* mutant phenotype (Sierro et al., 2007), but not with a subsequent independent *Cxcr7* knockout study (Gerrits et al., 2008). Perinatal lethality was observed in both studies. However, Gerrits et al. (2008) did not observe semilunar valve thickening or ventricular septal defects and concluded that the enlarged hearts in *Cxcr7*-null mice were due to hyperplasia. In contrast, Sierro et al. (2007) observed aortic and pulmonary valve thickening, as well as bicuspid aortic valves, a finding we did not observe. These discrepancies might reflect differences in genetic background, knockout strategies, or effects on neighboring genes. Gerrits et al. (2008) knocked in the β-galactosidase (LacZ) transgene in the place of *Cxcr7* exon2, while we and Sierro et al. (2007) replaced the exon2 with a *loxP*-flanked conditional allele.

Fig. 3. *Cxcr7*$^{-/-}$ embryos have enlarged semilunar valves and occasional VSD or overriding aorta. **A–J:** H&E-stained sections of E18.5 embryos. *Cxcr7*$^{-/-}$ embryos have thick pulmonary valve (PV) and aortic valves (AoV) but normal tricuspid and mitral valves. VSD was observed in 33% (n=9) of cases (arrow in I). Transverse sections are shown in A, C, F, and H. Coronal sections are shown in B, D, E, G, I, and J. Ao, aorta; PV, pulmonary valve; RV, right ventricle; LV, left ventricle; LA, left atrium; RA, right atrium; MV, mitral valve; TV, tricuspid valve. **K–R:** Coronal sections of hearts from wild-type and *Cxcr7*$^{-/-}$ embryos at various developmental stages. The sizes and cell numbers of OFT endocardial cushions or semilunar valves were not significantly different in wild-type and *Cxcr7*$^{-/-}$ embryos until E14. Difference in the size of semilunar valves became apparent at around E15.5, when the valves undergo a remodeling process and form thin leaflets in wild-type hearts, but remained enlarged in *Cxcr7*$^{-/-}$ hearts.

Fig. 4. Increased proliferation of cardiac semilunar valve mesenchymal cells in *Cxcr7* mutants. **A,B:** Cells undergoing mitosis were stained with pH3 antibody (red) at various embryonic stages. Nuclei were counterstained with DAPI (blue). There were more proliferating cells in semilunar valves in *Cxcr7*$^{-/-}$ embryos from E14 onward. Shown are representative sections at E15.5. **C:** Quantitative analysis of pH3 immunostaining (pH3-positive cells/total valve cells × 100) showed that the percentage of cells undergoing mitosis in *Cxcr7*$^{-/-}$ valves was increased ~2-fold at E14 and ~3.5-fold at E15.5. *$P < 0.01$.

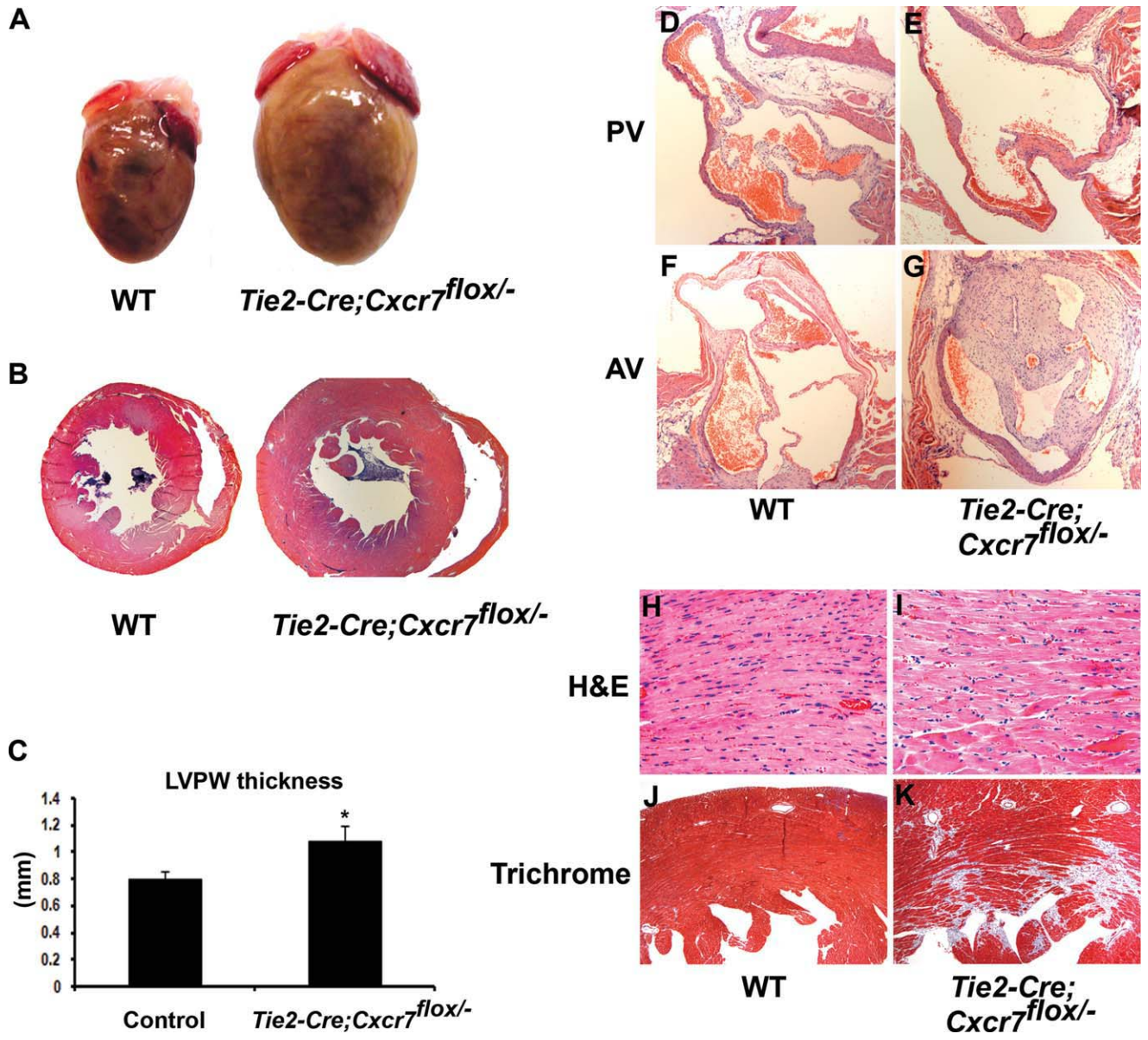

Fig. 5.

No predicted microRNAs are in this locus, making it less likely that there are differences in the deletion of potentially embedded genes.

Semilunar valve thickening in *Tie2-CreCxcr7*$^{flox/-}$ mice confirms the endothelial origin of this phenotype. However, the less severe phenotype of *Tie2-CreCxcr7*$^{flox/-}$ mice compared to germline *Cxcr7*$^{-/-}$ mice suggests that *Cxcr7* function in other cell types may also be important. Given the *Cxcr7* expression in neural crest–derived cushion mesenchymal cells and lack of overriding aorta and VSD in *Tie2-CreCxcr7*$^{flox/-}$ mice, *Cxcr7* may also have a critical function in neural crest–derived cushion cells during

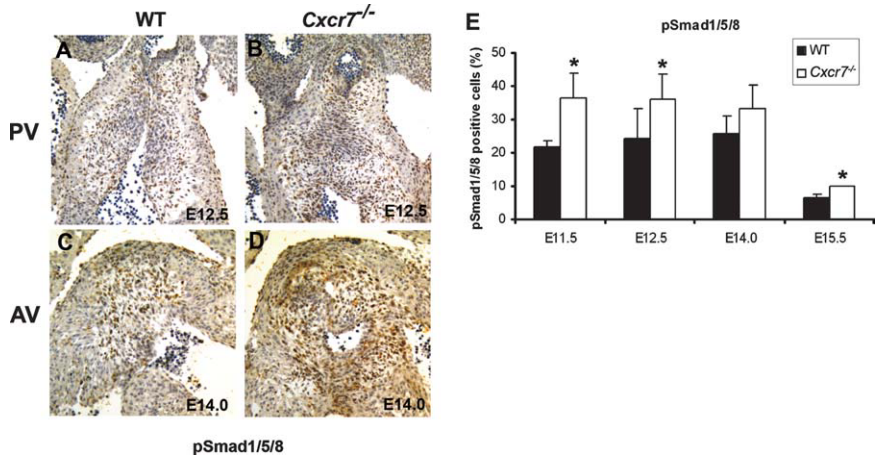

Fig. 6.

OFT maturation and septum formation. Alternatively, the imperfect recombination induced by *Tie2-Cre* might have prevented elicitation of the low penetrance VSD and overriding aorta (33 and 22%, respectively) phenotypes in *Tie2-CreCxcr7*$^{flox/-}$ mice. Further study is required to pinpoint the cellular origin of each phenotype and to elucidate the *Cxcr7* function in neural crest–derived cells using neural crest–specific *Cre* mice.

Disruption of EGFR signaling pathways in mice also causes cardiac valve hypertrophy due to increased proliferation at the late stage of valve development (Chen et al., 2000; Jackson et al., 2003). There is evidence that EGFR signaling antagonizes BMP signaling (Kretzschmar et al., 1997; Nonaka et al., 1999; Lo et al., 2001), and pSmad1/5/8 levels may be increased in *Hbegf* knockout valves (Jackson et al., 2003), consistent with a link between EGFR signaling and *Cxcr7*. EGFR activation antagonizes BMP signaling by phosphorylating Smad proteins at the linker region distinct from phosphorylation sites by BMP receptor (Kretzschmar et al., 1997) or by stabilizing the Smad transcriptional co-repressor TGIF (Lo et al., 2001). Both effects are mediated by the MAPK Erk. In one study, *Hbegf* mRNA was downregulated in *Cxcr7*$^{-/-}$ semilunar valves, corroborating the relationship between EGFR signaling and CXCR7 (Sierro et al., 2007). It is unclear how CXCR7 regulates *Hbegf* expression. In our study, treating CXCL12 to primary sheep aortic valve mesenchymal cells, which express *Cxcr7*, or *Cxcr7*-transfected COS1 cells did not activate EGFR signaling (data not shown).

CXCR7 shares the same ligand, CXCL12, with CXCR4 but ligand binding to CXCR7 does not activate classical chemokine pathways such as Ca^{2+} mobilization or MAPK signaling (Burns et al., 2006; Proost et al., 2007; Boldajipour et al., 2008; Hartmann et al., 2008). Although CXCR7 can modulate the function of CXCR4 through ligand sequestration or heterodimerization (Dambly-Chaudiere et al., 2007; Sierro et al., 2007; Valentin et al., 2007; Boldajipour et al., 2008; Levoye et al., 2009; Zabel et al., 2009), semilunar valve thickening is a unique phenotype of *Cxcr7* knockout mice that is not observed in either *Cxcr4* or *Cxcl12* knockout mice, where VSD is the major cardiac phenotype. In contrast, semilunar valve thickening is caused by both *Cxcr7* deficiency and disruption of EGFR signaling, although VSD and overriding aorta are unique to *Cxcr7*$^{-/-}$ mice. Thus, CXCR7 may influence semilunar valve morphogenesis and ventricular septum formation/OFT maturation through two separate mechanisms. It will be interesting to test whether CXCR7 activates different pathways in endocardial- and neural crest–derived cushion mesenchymal cells.

Valve defects are among the most common forms of human congenital heart disease and typically involve abnormal thickening of the aortic or pulmonary valves. The consequences can range from neonatal cardiac failure to cardiac hypertrophy later in life, depending on the severity of the stenosis. Numerous signaling pathways have been linked to valve formation (Armstrong and Bischoff, 2004). Disruption of any of these pathways during pregnancy could lead to fatal conditions, underscoring the importance of elucidating the exact mechanisms of valve formation. For example, the absence of *Ptpn11*, which is involved in a signaling pathway mediated by the EGFR, results in dysplastic outflow valves (Chen et al., 2000). In humans, mutations of *PTPN11*, which encodes the protein tyrosine phosphatase Shp-2, cause Noonan syndrome, characterized by pulmonic valve stenosis (Tartaglia et al., 2001). Similarly, human mutations in *NOTCH1* (Garg et al., 2005) cause thickened aortic valve leaflets and can result in aortic valve stenosis early or later in life. It will be interesting to determine whether CXCR7 or pathways that it regulates also contribute to human aortic or pulmonary valve disease.

EXPERIMENTAL PROCEDURES

Generation of Conditionally Targeted *Cxcr7* Mice

All experimental procedures were approved by the Institutional Animal Care and Use Committee at the University of California San Francisco. A conditional knockout targeting vector was designed to insert *loxP* sequences about 100–200 base pairs from either side of exon 2 of the *Cxcr7* locus. The linearized targeting vector was electroporated into 129/SvEv embryonic stem (ES) cells (Dr. B. Koller, University of North Carolina, Chapel Hill, NC). ES clones were screened by PCR and verified by Southern blot. Correctly targeted ES cells were injected into C57BL/6 mouse blastocysts. Chimeric offspring were crossed with C57BL/6 mice, and agouti offspring were screened for the targeted allele, *Cxcr7*^{flox}. *Deleter* Cre transgenic mice were used to allow Cre-mediated recombination in all cells (Schwenk et al., 1995). *Tie2-CreCxcr7*$^{flox/-}$ mice were generated by crosses of *Cxcr7*$^{flox/flox}$ × *Tie2-CreCxcr7*$^{+/-}$ or *Cxcr7*$^{flox/-}$ × *Tie2-CreCxcr7*$^{flox/+}$. *Tie2-*

Fig. 5. Endothelial-specific deletion of *Cxcr7* causes cardiac semilunar valve stenosis and secondary hypertrophy. **A:** Image of whole hearts taken from 6-month-old wild-type or *Tie2-CreCxcr7*$^{flox/-}$ mice. Endothelial-specific deletion of *Cxcr7* caused marked hypertrophy. **B:** Transverse sections of wild-type and *Tie2-CreCxcr7*$^{flox/-}$ mice. The mutant heart had a thicker ventricular wall than the wild-type heart but a similarly sized ventricular cavity. **C:** Left ventricular posterior wall (LVPW) thickness, measured by echocardiography, was ~1.4-fold thicker in *Tie2-CreCxcr7*$^{flox/-}$ hearts than in wild-type hearts (n=3 per group, $^*P<0.05$). **D–G:** Heart sections of 6-month-old wild-type or *Tie2-CreCxcr7*$^{flox/-}$ mice were stained with hematoxylin-eosin. *Tie2-CreCxcr7*$^{flox/-}$ mice had aortic valve (AoV) stenosis similar to that in *Cxcr7*$^{-/-}$ mice but a milder pulmonary valve (PV) phenotype. **H,I:** Magnified images (20×) of wild-type and *Tie2-CreCxcr7*$^{flox/-}$ heart sections stained with hematoxylin-eosin. Myocardial structure was disarrayed and the myocytes were not well packed in mutant hearts. **J,K:** Masson's trichrome staining showed more collagen deposition (blue) in *Tie2-CreCxcr7*$^{flox/-}$ hearts than in wild-type hearts.

Fig. 6. CXCR7 deficiency enhances BMP signaling in semilunar valves. **A–D:** Immunohistochemistry with anti-phospho-Smad1/5/8 (pSmad1/5/8) antibody (brown) shows increased BMP signaling in *Cxcr7*$^{-/-}$ semilunar valves. Nuclei were counterstained with hematoxylin. **E:** Quantitation of pSmad1/5/8 immunostaining shows that the BMP signaling was increased throughout cardiac valve development in *Cxcr7*$^{-/-}$ mice. $^*P < 0.05$.

CreCxcr7$^{flox/+}$ mice were used as wild-type controls. *Tie2-Cre* mice (Koni et al., 2001) were purchased from the Jackson Laboratory (West Grove, PA).

In Situ Hybridization

Section in situ hybridization for P1 mouse was performed by Phylogeny (Columbus, OH). Mouse tissue was frozen, cut into 6–12μm sections, mounted on gelatin-coated slides, and fixed in 4% formaldehyde. The cRNA probe for *Cxcr7* was synthesized in vitro according to the manufacturer's conditions (Ambion, Austin, TX) and labeled with ^{35}S-UTP (Amersham, Pittsburgh, PA). Sections were hybridized overnight at 55°C with ^{35}S-labeled cRNA probe (50–80,000 cpm/μl). Whole-mount in situ hybridization for *Cxcr7* and *Crabp* mRNAs was performed with E10.5–E11.0 embryos (n=4 and 3, respectively) as described (Kwon et al., 2009). Embryos were fixed in 4% formaldehyde overnight and kept in 100% methanol at −20°C until use. Hybridization was performed at 65°C overnight. Riboprobes were labeled with DIG, and embryos were stained according to the manufacturer's instruction (Roche, Indianapolis, IN).

Histology

Embryonic hearts at various stages were embedded in paraffin, cut into 8–10-μm sections, deparaffinized, and stained with hematoxylin and eosin for histological analysis (n=4 for E11.5, n=3 for E12.5, n=3 for E14.0, n=3 for E15.5, and n=4 for E18.5). For Masson's trichrome staining, 6-month-old hearts from wild-type and *Tie2-CreCxcr7*$^{flox/-}$ mice were embedded in paraffin and transversely sectioned (n=3 for each group). Deparaffinized sections were dipped sequentially into Weigert's iron hematoxylin working solution for 10 min, Biebrich scarlet-acid fuchsin solution for 15 min, phosphomolybdic-phosphotungstic acid solution for 15 min, aniline blue solution 5–10 min, and 1% acetic acid solution for 2–5 min.

Immunostaining and TUNEL Assay

Paraffin-embedded embryos of wild-type and *Cxcr7*$^{-/-}$ mice were cut at various stages either transversely or coronally. For immunostaining, antibodies for phospho-histone H3 (Upstate, East Syracuse, NY) and phospho-Smad1/5/8 (Cell Signaling, Danvers, MA) were used at 1:100 dilution. For pH3 staining, a FITC-conjugated secondary antibody was used, and the slides were mounted with Vectashield containing DAPI (Vector Laboratories, Burlingame, CA). For pSmad1/5/8 staining, a horseradish peroxidase–conjugated secondary antibody was used, and the sections were stained with the ABC staining system (Vector Laboratories). TUNEL assays were performed with an in situ cell death detection kit (Roche). Number of animals used: pH3 staining (n=3 for E11.5, E12.5, E13.5, and E14.0; n=5 for E15.5); pSmad1/5/8 staining (n=3 for E11.5 and E15.5, n=6 for E12.5 and E14.0); TUNEL assay (n=2 for E11.5, n=3 for E12.5, n=4 for E14.0 and E15.5). For wild-type and mutant mice, the same numbers of animals were used.

Echocardiography

Systolic function and ventricular wall thickness were assessed with M-mode and power Doppler mode in 6-month-old wild-type and *Tie2-CreCxcr7*$^{flox/-}$ mice (n=3 for each group); mice were anesthetized with 1.75% isoflurane. Core temperature was maintained at 37–38°C, and scans were performed in a random-blind fashion. Each mouse underwent three separate scans on three different days. Values were averaged from three scans.

Statistical Analysis

Statistical analysis was performed with the Student's *t*-test and $P < 0.05$ was considered statistically significant.

REFERENCES

Armstrong EJ, Bischoff J. 2004. Heart valve development: endothelial cell signaling and differentiation. Circ Res 95: 459–470.

Balabanian K, Lagane B, Infantino S, Chow KY, Harriague J, Moepps B, Arenzana-Seisdedos F, Thelen M, Bachelerie F. 2005. The chemokine SDF-1/CXCL12 binds to and signals through the orphan receptor RDC1 in T lymphocytes. J Biol Chem 280: 35760–35766.

Boldajipour B, Mahabaleshwar H, Kardash E, Reichman-Fried M, Blaser H, Minina S, Wilson D, Xu Q, Raz E. 2008. Control of chemokine-guided cell migration by ligand sequestration. Cell 132: 463–473.

Burns JM, Summers BC, Wang Y, Melikian A, Berahovich R, Miao Z, Penfold ME, Sunshine MJ, Littman DR, Kuo CJ, Wei K, McMaster BE, Wright K, Howard MC, Schall TJ. 2006. A novel chemokine receptor for SDF-1 and I-TAC involved in cell survival, cell adhesion, and tumor development. J Exp Med 203:2201–2213.

Chen B, Bronson RT, Klaman LD, Hampton TG, Wang JF, Green PJ, Magnuson T, Douglas PS, Morgan JP, Neel BG. 2000. Mice mutant for Egfr and Shp2 have defective cardiac semilunar valvulogenesis. Nat Genet 24:296–299.

Dambly-Chaudiere C, Cubedo N, Ghysen A. 2007. Control of cell migration in the development of the posterior lateral line: antagonistic interactions between the chemokine receptors CXCR4 and CXCR7/RDC1. BMC Dev Biol 7:23.

Gerrits H, van Ingen Schenau DS, Bakker NE, van Disseldorp AJ, Strik A, Hermens LS, Koenen TB, Krajnc-Franken MA, Gossen JA. 2008. Early postnatal lethality and cardiovascular defects in CXCR7-deficient mice. Genesis 46:235–245.

Hartmann TN, Grabovsky V, Pasvolsky R, Shulman Z, Buss EC, Spiegel A, Nagler A, Lapidot T, Thelen M, Alon R. 2008. A crosstalk between intracellular CXCR7 and CXCR4 involved in rapid CXCL12-triggered integrin activation but not in chemokine-triggered motility of human T lymphocytes and CD34+ cells. J Leukoc Biol 84:1130–1140.

Heesen M, Berman MA, Charest A, Housman D, Gerard C, Dorf ME. 1998. Cloning and chromosomal mapping of an orphan chemokine receptor: mouse RDC1. Immunogenetics 47:364–370.

Hutson MR, Kirby ML. 2003. Neural crest and cardiovascular development: a 20-year perspective. Birth Defects Res C Embryo Today 69:2–13.

Hutson MR, Kirby ML. 2007. Model systems for the study of heart development and disease. Cardiac neural crest and conotruncal malformations. Semin Cell Dev Biol 18:101–110.

Jackson LF, Qiu TH, Sunnarborg SW, Chang A, Zhang C, Patterson C, Lee DC. 2003. Defective valvulogenesis in HB-EGF and TACE-null mice is associated with aberrant BMP signaling. Embo J 22:2704–2716.

Jessup M, Brozena S. 2003. Heart failure. N Engl J Med 348:2007–2018.

Kalatskaya I, Berchiche YA, Gravel S, Limberg BJ, Rosenbaum JS, Heveker N. 2009. AMD3100 is a CXCR7 ligand

with allosteric agonist properties. Mol Pharmacol 75:1240–1247.
Koni PA, Joshi SK, Temann UA, Olson D, Burkly L, Flavell RA. 2001. Conditional vascular cell adhesion molecule 1 deletion in mice: impaired lymphocyte migration to bone marrow. J Exp Med 193:741–754.
Kretzschmar M, Doody J, Massague J. 1997. Opposing BMP and EGF signalling pathways converge on the TGF-beta family mediator Smad1. Nature 389:618–622.
Kwon C, Qian L, Cheng P, Nigam V, Arnold J, Srivastava D. 2009. A regulatory pathway involving Notch1/beta-catenin/Isl1 determines cardiac progenitor cell fate. Nat Cell Biol 11:951–957.
Levoye A, Balabanian K, Baleux F, Bachelerie F, Lagane B. 2009. CXCR7 heterodimerizes with CXCR4 and regulates CXCL12-mediated G protein signaling. Blood 113:6085–6093.
Lo RS, Wotton D, Massague J. 2001. Epidermal growth factor signaling via Ras controls the Smad transcriptional corepressor TGIF. Embo J 20:128–136.
Ma Q, Jones D, Borghesani PR, Segal RA, Nagasawa T, Kishimoto T, Bronson RT, Springer TA. 1998. Impaired B-lymphopoiesis, myelopoiesis, and derailed cerebellar neuron migration in CXCR4- and SDF-1-deficient mice. Proc Natl Acad Sci USA 95:9448–9453.
Madden SL, Cook BP, Nacht M, Weber WD, Callahan MR, Jiang Y, Dufault MR, Zhang X, Zhang W, Walter-Yohrling J, Rouleau C, Akmaev VR, Wang CJ, Cao X, St Martin TB, Roberts BL, Teicher BA, Klinger KW, Stan RV, Lucey B, Carson-Walter EB, Laterra J, Walter KA. 2004. Vascular gene expression in nonneoplastic and malignant brain. Am J Pathol 165:601–608.
Miao Z, Luker KE, Summers BC, Berahovich R, Bhojani MS, Rehemtulla A, Kleer CG, Essner JJ, Nasevicius A, Luker GD, Howard MC, Schall TJ. 2007. CXCR7 (RDC1) promotes breast and lung tumor growth in vivo and is expressed on tumor-associated vasculature. Proc Natl Acad Sci USA 104: 15735–15740.
Nagasawa T, Hirota S, Tachibana K, Takakura N, Nishikawa S, Kitamura Y, Yoshida N, Kikutani H, Kishimoto T. 1996. Defects of B-cell lymphopoiesis and bone-marrow myelopoiesis in mice lacking the CXC chemokine PBSF/SDF-1. Nature 382:635–638.
Nonaka K, Shum L, Takahashi I, Takahashi K, Ikura T, Dashner R, Nuckolls GH, Slavkin HC. 1999. Convergence of the BMP and EGF signaling pathways on Smad1 in the regulation of chondrogenesis. Int J Dev Biol 43:795–807.
Proost P, Mortier A, Loos T, Vandercappellen J, Gouwy M, Ronsse I, Schutyser E, Put W, Parmentier M, Struyf S, Van Damme J. 2007. Proteolytic processing of CXCL11 by CD13/aminopeptidase N impairs CXCR3 and CXCR7 binding and signaling and reduces lymphocyte and endothelial cell migration. Blood 110:37–44.
Raggo C, Ruhl R, McAllister S, Koon H, Dezube BJ, Fruh K, Moses AV. 2005. Novel cellular genes essential for transformation of endothelial cells by Kaposi's sarcoma-associated herpesvirus. Cancer Res 65:5084–5095.
Schwenk F, Baron U, Rajewsky K. 1995. A cre-transgenic mouse strain for the ubiquitous deletion of loxP-flanked gene segments including deletion in germ cells. Nucleic Acids Res 23: 5080–5081.
Sierro F, Biben C, Martinez-Munoz L, Mellado M, Ransohoff RM, Li M, Woehl B, Leung H, Groom J, Batten M, Harvey RP, Martinez AC, Mackay CR, Mackay F. 2007. Disrupted cardiac development but normal hematopoiesis in mice deficient in the second CXCL12/SDF-1 receptor, CXCR7. Proc Natl Acad Sci USA 104:14759–14764.
Snarr BS, Kern CB, Wessels A. 2008. Origin and fate of cardiac mesenchyme. Dev Dyn 237:2804–2819.
Stoller JZ, Epstein JA. 2005. Cardiac neural crest. Semin Cell Dev Biol 16: 704–715.
Tachibana K, Hirota S, Iizasa H, Yoshida H, Kawabata K, Kataoka Y, Kitamura Y, Matsushima K, Yoshida N, Nishikawa S, Kishimoto T, Nagasawa T. 1998. The chemokine receptor CXCR4 is essential for vascularization of the gastrointestinal tract. Nature 393: 591–594.
Tartaglia M, Mehler EL, Goldberg R, Zampino G, Brunner HG, Kremer H, van der Burgt I, Crosby AH, Ion A, Jeffery S, Kalidas K, Patton MA, Kucherlapati RS, Gelb BD. 2001. Mutations in PTPN11, encoding the protein tyrosine phosphatase SHP-2, cause Noonan syndrome. Nat. Genet. 29: 465–468.
Valentin G, Haas P, Gilmour D. 2007. The chemokine SDF1a coordinates tissue migration through the spatially restricted activation of Cxcr7 and Cxcr4b. Curr Biol 17:1026–1031.
Zabel BA, Wang Y, Lewen S, Berahovich RD, Penfold ME, Zhang P, Powers J, Summers BC, Miao Z, Zhao B, Jalili A, Janowska-Wieczorek A, Jaen JC, Schall TJ. 2009. Elucidation of CXCR7-mediated signaling events and inhibition of CXCR4-mediated tumor cell transendothelial migration by CXCR7 ligands. J Immunol 183:3204–3211.
Zou YR, Kottmann AH, Kuroda M, Taniuchi I, Littman DR. 1998. Function of the chemokine receptor CXCR4 in haematopoiesis and in cerebellar development. Nature 393:595–599.